LIDAR-DERIVED SOIL COMPACTION USING DEPLOYABLE PROBES AND SHORT-WAVE IR RETRO-REFLECTORS

Dr. John Anderson, Dr. Richard Massaro, and Jarrod Edwards
US Army Engineer Research and Development Center
7701 Telegraph Road, Alexandria, VA 22315

Dr. Kevin Slocum and Dave Kalin
National Geospatial Intelligence Agency (NGA)
4600 Sangamore Road, Bethesda, MD 20816

ABSTRACT

Military operations associated with activities such as mobility and landing zone placement depend on accurate information related to terrain morphology and soil characteristics. LIDAR has provided a way to derive timely, high-resolution terrain maps that represent accurate topographic information, but fall short in the derivation of actual terrain feature condition as it relates to soils (e.g., compaction, moisture). We present in this paper a proposed technique and model for deployable soil penetrometers incorporating a new generation of short-wave infrared retro-reflective optics for the determination of soil compaction. As a terrain metric, soil compaction is directly related to composition and water potential. These two factors and their association with topographic landscape position provide military planners a more detailed account of soil properties than topography alone. The use of highly efficient retro-reflective optics with a steerable, short-wave IR LIDAR (1064 nm or 1550 nm) permits the determination of soil compaction as a function of penetrometer elevation and depth. Our simple model incorporates terms related to the known reflectance return of the retro-reflector, length of the penetrometer and the difference in the depth of deployed penetrometers related to the ground to determine a compaction value. This value is ultimately used as a calibration metric for judging binary-soft versus hard - soil conditions based on compaction.

KEY WORDS: LIDAR, Soils, Penetrometer, Soil Compaction, Retro-Reflector

INTRODUCTION

Soil compaction (SC) is a research topic of high interest that extends beyond the agricultural community into environmental impacts and assessment of other civil and military activities. Military operations associated with activities such as mobility and landing zone placement depend on accurate information related to terrain morphology and soil characteristics. LIDAR has provided a way to derive timely, high-resolution terrain maps that represent accurate topographic information, but fall short in the derivation of actual terrain feature condition as it relates to soils (e.g., compaction, moisture). For example, approaches for assessing the extent and influence of military vehicle traffic on natural areas are of high interest to the ERDC and military in general [1]. Numerous ground techniques have been developed and employed for characterizing the spatial variability of SC, relating it to other soil physical features, and often using integrative sensor approaches. These traditional methods for direct measures of SC are labor-demanding and time-consuming, and there is a critical need therefore for alternative approaches to conducting large-scale field mapping [2-4]. Studies linking SC patterns to remotely sensed data are limited, and to the best of our knowledge have never involved the use of soil probes detectable and interpretable from significant standoff distances. Further, the use of highly efficient, well designed LIDAR ground targets is critical for accurate assessment of intensity, spatial and elevation (height) attributes [5].

We have recognized two fundamental issues exist in remote compaction measurements using probes: 1) design of the instrument itself modeled on the penetrometer, robust enough to be deployed from an aircraft at intervals for meaningful interpolation and 2) the ultimate optical recovery of deployed probes in a complex and varied LiDAR scene. In this paper we describe a comparative study of emerging materials for use with LiDAR systems operating in the short-wave infrared region (e.g., 1064 nm, 1550 nm). These materials include coated barium titanate glass beads incorporated on model penetrometers. These materials were selected for their remarkable refractive indices and the potential incident signal they would return within a LiDAR point cloud. While the use of retro-reflective

optics is not new, the development of novel coatings and sizing within the micron region has greatly improved the signal-to-noise efficiency, versatility and wavelength selectivity afforded by these materials.

METHODS

Soil Penetrometers

The evaluation of deployed probes was accomplished during an experiment incorporating a pointable airborne LiDAR. These experiments took place in late Summer 2009 along the Potomac River, near Colonial Beach, Virginia (38º 18' 06.47 N and 77º 01' 05.52 W). Model penetrometers were deployed in upland and wetland areas to provide a measure of compaction along topographic and environmental boundaries. The goals were: 1) to collect field penetrometer data (in psi units) on the soils and 2) use this as a basis for depth placement of the model penetrometers and 3) situate them in such a way to analyze recovery based on retro-reflective return. The model probe design consisted of a 1.27 cm diameter pvc tube 100 cm long with a detachable reflective end that was 12 cm in diameter. This size was selected to ensure that the area was slightly larger than the range resolution of the LiDAR (i.e., 5 to 10 cm). Barium titanate ($BaTiO_3$) glass beads were used in an adhesive matrix to coat the probe ends. The probes were deployed level and nadir to the LiDAR FOV.

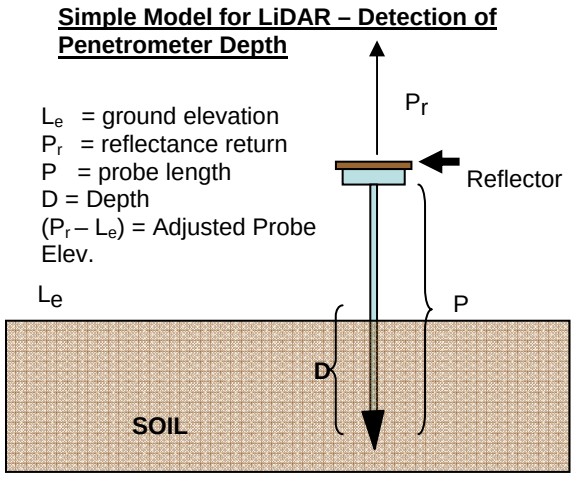

Figure 1. Schematic of deployable soil penetrometer.

Retro Reflectors

In our selection of BaTiO3 glass beads, a theoretical model of their retro-reflective properties, (i.e., their ability to reflect light back along the direction of the incident illuminating beam) was applied. Since the probe area presented to the LiDAR excitation is only 12 cm in diameter, the retroreflective properties of the beads was a critical

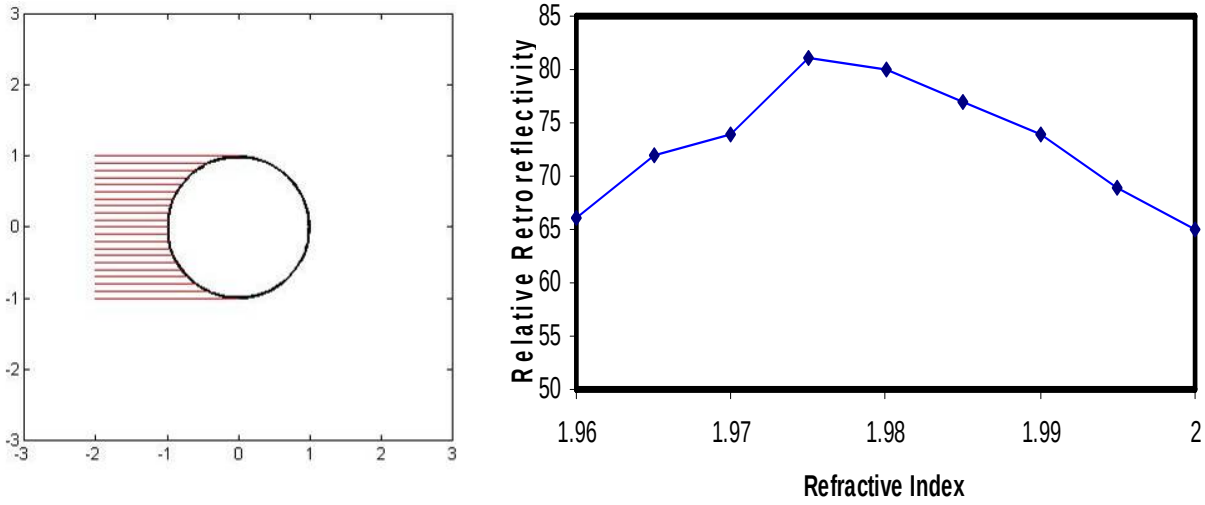

Figure 2A and 2B. Uniform light impinging on a retroreflective bead and a model of retroreflective efficiency as a function of refractive index. (models courtesy Dr. Richard Moyers, ORNL)

factor in predicting the necessary return against a complex background. The retroreflective properties were

evaluated as a function of the bead refractive index, internal specular reflection in accordance with Snell's law, and diffuse reflection from a coating on the wall of the bead. Given a uniform ray of light propagating parallel to the x-axis is incident on a single sphere, as shown in Figure 2A. Light incident on the surface of the sphere will behave in accordance with Snell's law:

EQ1.

$$\eta_i \sin\theta_i = \eta_t \sin\theta_t$$

where $\boldsymbol{\eta_i}$ is the index of refraction of the incident medium (air, $\boldsymbol{\eta_i = 1}$), and $\boldsymbol{\eta_t}$ is the index of refraction inside the bead. $\boldsymbol{\Theta_i}$ is the angle of the incident light relative to the sphere surface normal, and $\boldsymbol{\Theta_t}$ is the angle of the refracted beam. Snell's law predicts that some of the incident light will be reflected by the front surface of the sphere, and the rest will be refracted toward the rear surface. Light that reaches the rear surface will again experience reflectance and refraction at the surface. Most of the light is transmitted out of the bead, but about 15% of the light will be reflected off of the surface back toward the front surface of the bead. The model indicates that, depending on the refractive index, 9% - 12% of the light originally incident upon the bead will be transmitted out of the sphere and retroreflected back towards the incident light source. A plot of retoreflected intensity as a function of bead refractive index is shown in Figure 2B. The plot shows that the model indicates that a bead index of 1.977 should provide optimal retroreflectivity and thus be easily recovered in a complex point cloud representing a variety of terran features.

LiDAR

The LIDAR sensor used for this experiment was a modified Optech ALTM 3100/Gemini LIDAR system. The system operates between 33 to 167 kHz pulse repetition rate (33000 to 167000 light pulses per second) and at a variety of altitudes ranging from 800 to 3500m. The scan rate, pulse rate, and altitude were chosen to achieve a variety of independent point spacing (i.e., resolution) on the ground. The data collected for this paper was captured using the ALTM's four channel, analog timing measurement circuit, which was capable of recording four returns for each transmitted laser pulse (first, second, third, and last). The airborne platform used in this experiment was a King Air A90 aircraft operated by Dynamic Aviation, Staunton, Virginia. The ALTM was mounted inside the aircraft to enable a standard nadir mapping function. This allowed an unobstructed field of view (FOV) of +/- 20 degrees, which is consistent with the scan mirror range of the LIDAR sensor. To enable target mode collection, the sensor was mounted in a JHU APL designed two-axis gimbal with a stabilized pointing system. This gimbal can provide an additional +/- 30 degrees of motion about each axis when mounted in a King Air A90 aircraft.

The normal, minimum eye safe operating altitude is 640 m, AGL. For our tests, we started with an altitude of 171 m, AGL to get as much laser energy on the ground as possible. This required that the test be performed on the Laser Range and all personnel wear laser eye protection. To further maximize the laser energy per pulse, the system was operated at the minimum laser pulse rate of 33 kHz and in target mode where a small area of ground (50 x 50 m) was continuously scanned as the plane flew overhead at a nominal speed of 68 m/s. Thirty-one passes comprised the test sortie with altitudes of 171, 201, 238, 274, and 335 m, AGL.

Deploying Soil Probes

Probe deployment followed the guidelines and procedures developed by Colorado State University for sampling soil compaction using hand-held soil penetrometers [6]. To place the probes, a static, digital penetrometer was used that required a fixed pressure to drive the cone into the ground not to exceed a depth of 80 cm. The penetrometer we used employed a shaft 80 cm long and incorporated a 30º cone. For each probe, the related pressure was recorded, as was the depth of penetration into the soil. The pressure limit for the instrument was fixed at 200 psi, so soil compaction requiring more force for the cone penetration would be limited in depth of penetration. Once the soil was tested, the deployable probe was inserted and leveled into the sampling hole (figure 3). Recalibration of the penetrometer instrument was conducted between each deployment to compensate for variations in pressure between operators and soil conditions. Table one shows the soil types, psi, and depths associated with probe placement.

Figure 3. Deploying model penetrometers.

RESULTS

The recovery of penetrometers by LiDAR yielded good results. The pointable LiDAR (+/- 30º) produced dense point cloud development over areas of probe placement, thusmaking optical recovery successful. The high return afforded by the retroreflectors stood out against the background, presenting a pseudo elevation in the range and a strong return in the intensity data. Both sets of data were analyzed to find the probes and then query their elevations to profile the soil conditions against the topographic surface. These results are shown below:

Table 1. Probe Number, PSI and Soil Description, and Depth (cm).

PROBE ID	PSI / Soil	DEPTH (cm)
1	40 / humic	18 cm
2	45 / humic	19 cm
3	175 / sand + gravel	10 cm
4	180 / sand + gravel	12 cm
5	190 / hard gravel fill	8 cm
6	190 / hard gravel fill	10 cm
7	140 / sand	50 cm
8	140 sand	50 cm

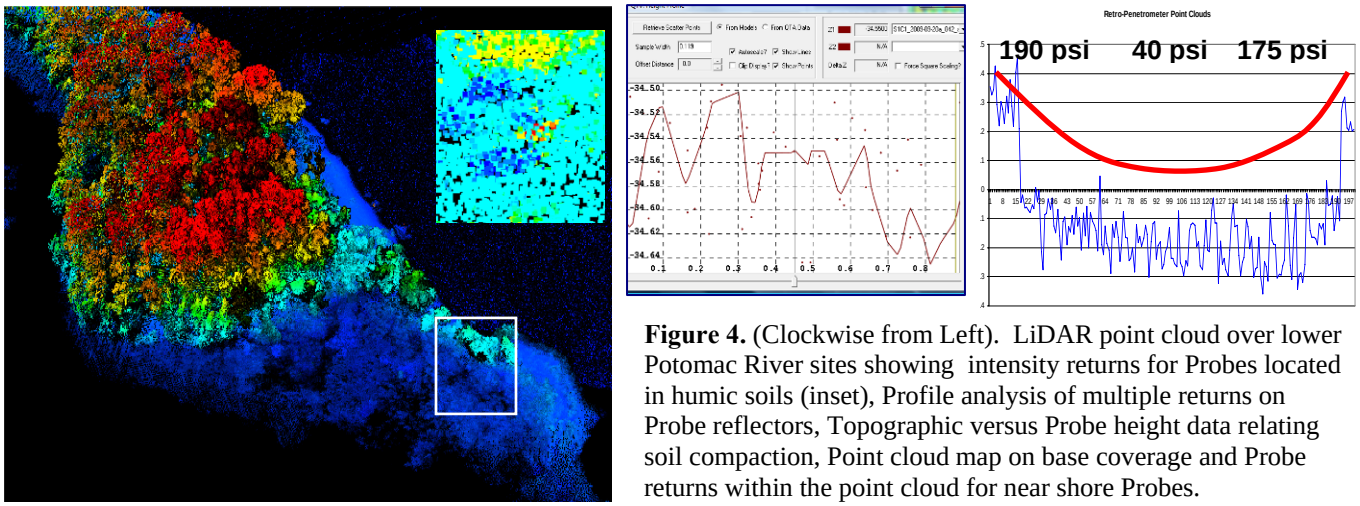

Figure 4. (Clockwise from Left). LiDAR point cloud over lower Potomac River sites showing intensity returns for Probes located in humic soils (inset), Profile analysis of multiple returns on Probe reflectors, Topographic versus Probe height data relating soil compaction, Point cloud map on base coverage and Probe returns within the point cloud for near shore Probes.

CONCLUSIONS

For the recovered probes, it appears there is a logical soil compaction pattern that tracks well with the topographic surface (as seen in the above plot). The height information reveals soil conditions useful to trafficability as a function of related probe height and associated penetration. The next phase of this research will be to develop a deployable probe modeled on a dynamic design where a sliding hammer is used to apply more equal force to the cone to accomplish more consistent measurements. These would be dropped from fixed or rotary wing aircraft at known heights. The derivation of soil condition would be similar to this experiment, based on retroreflective return and height difference, however, a more complex penetrometer model based upon semi-empirical metrics (e.g., depth, clay content, bulk density, gravimetric moisture content) will be used [7].

In such complex and varied point clouds, the ability to detect the probes could not have been accomplished without the aid of high refractive index retroreflectors. The incident return of these materials to the LiDAR sensor made discovery easier, especially during analysis that included stripping the closest returns from the data to reveal reurns associated with the mid-canopy and ground. The emergence of these materials provides a useful tool to incorporate with LiDAR to accomplish more active remote sensing.

REFERENCES

Anderson, A.B., A.J. Palazzo, et al. Assessing the impacts of military vehicle traffic on natural areas: Introduction to the special issue and review of the relevant military vehicle impact literature, *J. Terramechanics*, **42**(3-4): 143-158.

Hemmat, A., and V.I. Adamchuk, 2008. Sensor systems for measuring soil compaction: Review and analysis, *Comput. Electron. Agr.*, **63**(2): 89-103.

Tekin, Y., B. Kul, and R. Okursoy, 2008. Sensing and 3D mapping of soil compaction, *Sensors*, **8**: 3447-3459.

Yurui, S., P.S. Lammers, et al., 2008. Determining soil physical properties by multi-sensor technique, *Sensor, Actuat. A: Phys.*, **147**(1): 352-357.

Csanyi, N., and C.K. Toth, 2007. Improvement of lidar data accuracy using lidar-specific ground targets, *PE&RS*, **73**(4): 385-396.

Jones, D., and M. Kunze, 2004. Guide to Sampling Soil Compaction Using Hand-Held Soil Penetrometers, Colorado State University Center for Environmental Management of Military Lands publication CEMML-TPS 04-1. Fort Collins, CO.

Canarache, A., 1990. PENETR – a generalized semi-empirical model estimating soil resistance to penetration, *Soil and Tillage Research*, **16:**51-70.